Nonlinear Dyn (2010) 62: 967–987
DOI 10.1007/s11071-010-9778-3

ORIGINAL PAPER

Shear deformable bars of doubly symmetrical cross section under nonlinear nonuniform torsional vibrations—application to torsional postbuckling configurations and primary resonance excitations

E.J. Sapountzakis · V.J. Tsipiras

Received: 13 January 2010 / Accepted: 6 July 2010 / Published online: 31 July 2010

Abstract In this paper a boundary element method is developed for the nonuniform torsional vibration problem of bars of arbitrary doubly symmetric constant cross section, taking into account the effects of geometrical nonlinearity (finite displacement—small strain theory) and secondary twisting moment deformation. The bar is subjected to arbitrarily distributed or concentrated conservative dynamic twisting and warping moments along its length, while its edges are subjected to the most general axial and torsional (twisting and warping) boundary conditions. The resulting coupling effect between twisting and axial displacement components is also considered and a constant along the bar compressive axial load is induced so as to investigate the dynamic response at the (torsional) postbuckled state. The bar is assumed to be adequately laterally supported so that it does not exhibit any flexural or flexural–torsional behavior. A coupled nonlinear initial boundary value problem with respect to the variable along the bar angle of twist and to an independent warping parameter is formulated. The resulting equations are further combined to yield a single partial differential equation with respect to the angle of twist. The problem is numerically solved employing the Analog Equation Method (AEM), a BEM based method, leading to a system of nonlinear Differential–Algebraic Equations (DAE). The main purpose of the present contribution is twofold: (i) comparison of both the governing differential equations and the numerical results of linear or nonlinear free or forced vibrations of bars ignoring or taking into account the secondary twisting moment deformation effect (STMDE) and (ii) numerical investigation of linear or nonlinear free vibrations of bars at torsional postbuckling configurations. Numerical results are worked out to illustrate the method, demonstrate its efficiency and wherever possible its accuracy.

Keywords Shear deformation · Secondary twisting moment deformation effect · Independent warping parameter · Bar · Beam · Boundary element method · Nonuniform torsion · Nonlinear vibrations · Torsional vibrations · Torsional postbuckling · Primary resonance

E.J. Sapountzakis (✉) · V.J. Tsipiras
Institute of Structural Analysis and Aseismic Research,
School of Civil Engineering,
National Technical University of Athens,
Zografou Campus, 157 80 Athens, Greece
e-mail: cvsapoun@central.ntua.gr

V.J. Tsipiras
e-mail: tsipiras@gmail.com

1 Introduction

When arbitrary torsional boundary conditions are applied either at the edges or at any other interior point of a bar due to construction requirements, this bar under the action of general twisting loading is leaded to nonuniform torsion. In this case, apart from the

well-known primary (St. Venant) shear stress distribution, normal and secondary (warping) shear stresses arise formulating the warping moment (bimoment) and secondary twisting moment (bishear), respectively [1, 2]. Warping shear stresses can be estimated by formulating a boundary value problem with respect to a secondary warping function [1, 3, 4] or by studying the equilibrium equations of a small segment of an elementary slice of the bar [5]. However, the aforementioned techniques do not achieve to include the warping shear stresses in the global equilibrium of the bar and to perform an accurate analysis of bars of closed shaped cross sections [6], that is to account for the secondary twisting moment deformation effect (STMDE). This effect generally necessitates the use of an independent warping parameter in the kinematical components of the bar (along with the angle of twist), increasing the difficulty of the problem at hand.

Besides, since weight saving is of paramount importance in many engineering fields, frequently used thin-walled open sections have low torsional stiffness and their torsional deformations may be of such magnitudes that it is not adequate to treat the angles of cross section rotation as small. In these cases, the study of nonlinear effects on these members becomes essential, where this nonlinearity results from retaining the nonlinear terms in the strain–displacement relations (finite displacement—small strain theory). When finite twist rotation angles are considered, the nonuniform torsional dynamic analysis of bars becomes much more complicated, leading to the formulation of coupled and nonlinear torsional and axial equations of motion. When the twist rotation angles of a member are small, a wide range of linear analysis tools, such as modal analysis, can be used and some analytical results are possible. As these rotation angles become larger, the induced geometrical nonlinearities result in effects that are not observed in linear systems. In such situations the possibility of an analytical solution method is significantly reduced and is restricted to special cases of boundary conditions or loading.

During the past few years, the *linear* static and linear free vibration analysis of *shear deformable bars* undergoing twisting or general deformations have been thoroughly studied [6–20] and theoretical statements and/or numerical comparisons between beam theories ignoring or taking into account the STMDE have been presented [6, 7, 9, 10, 19]. However, this is not the case for vibration analysis of bars taking into account both shear effects and geometrical nonlinearities. Cortinez and Piovan [21] and Machado and Cortinez [22] performed buckling and vibration analysis of composite beams of open and closed cross sections with orthotropic laminates, Minghini et al. [23] analyzed pultruded FRP beams and frames by developing locking-free elements while Vo and Lee [24] performed buckling and vibration analysis of composite beams of open cross sections with arbitrary lay ups. However, in the aforementioned contributions the analyzed cross sections are thin-walled ones, forced vibrations are not investigated and geometrical nonlinearities are considered only for static initial stresses and deformations.

During the past few years, the *nonlinear nonuniform torsional dynamic analysis* of bars has received a good amount of attention in the literature. Apart from research efforts that neglect torsional warping (Da Silva in [25, 26], Pai and Nayfeh in [27–29]), Di Egidio et al. in [30, 31] presented a FEM solution to the nonlinear flexural-torsional vibrations of thin-walled open beams taking into account in-plane and out-of-plane warpings and neglecting warping inertia. In these papers, the torsional–extensional coupling is taken into account but the inextensionality assumption leads to the fact that the axial boundary conditions are not general. Moreover, Simo and Vu-Quoc in [2] presented a FEM solution to a fully nonlinear (small or large strains, hyperelastic material) three-dimensional rod model based on a geometrically exact description of the kinematics of deformation. Pai and Nayfeh in [32] studied a geometrically exact nonlinear curved beam model for solid composite rotor blades using the concept of local engineering stress and strain measures and taking into account the in-plane and out-of-plane warpings. In the last two research efforts, the out-of-plane buckling of a framed structure and a helical spring have been analyzed respectively, thus the extensional–torsional coupling is not discussed. Recently, Avramov et al. [33] analyzed flexural–flexural–torsional free vibrations of twisted rotating beams employing nonlinear normal modes. Rozmarynowski and Szymczak [34] and Sapountzakis and Tsipiras [35] focus to the problem of nonlinear torsional vibrations. Nevertheless, dynamic analysis of bars at a torsional *postbuckled state*, as this is presented for the static case in [36], is not performed. Although free or forced vibrations of bars at flexural postbuckling configurations are well studied both numerically and experimentally [37–40], however this is not the case for

buckled bars at a torsional postbuckled state. To the authors' knowledge, only Mohri et al. [41] proposed a FEM solution to the linear free vibration analysis of pre- and postbuckled open thin-walled cross section beams subjected to special boundary conditions, neglecting warping inertia. In all of these research efforts the angle of twist per unit length is considered as a warping parameter with the exception of the aforementioned research effort of Simo and Vu-Quoc [2] who employed an independent one.

In this paper a boundary element method is developed for the nonuniform torsional vibration problem of bars of arbitrary doubly symmetric constant cross section, taking into account the effects of geometrical nonlinearity (finite displacement—small strain theory) and secondary twisting moment deformation. The bar is subjected to arbitrarily distributed or concentrated conservative dynamic twisting and warping moments along its length, while its edges are subjected to the most general axial and torsional (twisting and warping) boundary conditions. The resulting coupling effect between twisting and axial displacement components is also considered and a constant along the bar compressive axial load is induced so as to investigate the dynamic response at the (torsional) postbuckled state. The bar is assumed to be adequately laterally supported so that it does not exhibit any flexural or flexural—torsional behavior. A coupled nonlinear initial boundary value problem with respect to the variable along the bar angle of twist and to an independent warping parameter is formulated. The resulting equations are further combined to yield a single partial differential equation with respect to the angle of twist. The problem is numerically solved employing the Analog Equation Method [42], a BEM based method, leading to a system of nonlinear Differential–Algebraic Equations (DAE). The essential features and novel aspects of the present formulation compared with previous ones are summarized as follows.

i. The cross section is an arbitrarily shaped doubly symmetric thin or thick walled one. The formulation does not stand on the assumptions of a thin-walled structure and therefore the cross section's torsional and warping rigidities are evaluated "exactly" in a numerical sense.
ii. The beam is supported by the most general boundary conditions including elastic support or restraint.
iii. The trigonometric terms of the cross sectional twisting rotations appearing in the displacement field are retained without employing any simplifying approximations.
iv. The present investigation focuses to torsional vibrations and provides a unified framework for the theoretical statement and numerical comparison between shear deformable and shear undeformable bars undergoing linear or nonlinear, free of forced vibrations.
v. Nonlinear free vibrations at torsional postbuckling configurations and primary resonance excitations are numerically examined (in the second part of this contribution) revealing several aspects of nontrivial nonlinear phenomena.
vi. The adopted numerical procedure can efficiently analyze torsional vibrations of bars at postbuckling configurations without employing any assumptions on the form of the modeshapes of deformation.
vii. The proposed method employs a BEM approach (requiring boundary discretization exclusively for the cross sectional analysis) resulting in line or parabolic elements instead of area elements of the FEM solutions (requiring the whole cross section to be discretized into triangular or quadrilateral area elements), while a small number of line elements are required to achieve high accuracy.

2 Statement of the problem

2.1 Displacements, strains, stresses

Let us consider a prismatic bar of length l (Fig. 1), of constant arbitrary doubly symmetric cross section of area A. The homogeneous isotropic and linearly elastic material of the beam cross section, with modulus of elasticity E, shear modulus G and mass density ρ occupies the two-dimensional multiply connected region Ω of the y, z plane and is bounded by the Γ_j $(j = 1, 2, \ldots, K)$ boundary curves, which are piecewise smooth, i.e. they may have a finite number of corners. In Fig. 1a S_{yz} is the principal bending coordinate system through the cross section's shear center. The bar is subjected to the combined action of the arbitrarily distributed or concentrated time dependent conservative axial load $n(x, t)$ and twisting $m_t = m_t(x, t)$ and warping $m_w = m_w(x, t)$ moments acting in the

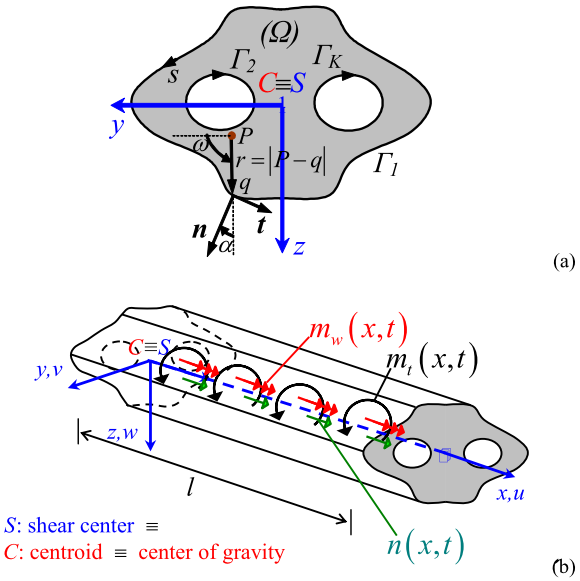

Fig. 1 Prismatic bar of an arbitrarily shaped doubly symmetric constant cross section occupying region Ω (**a**) subjected to axial and torsional loading (**b**)

x direction (Fig. 1b). The bar is assumed to be adequately laterally supported so that it does not exhibit any flexural or flexural—torsional behavior.

Under the aforementioned loading, the displacement field of the bar accounting for large twisting rotations is assumed to be given as

$$u(x,y,z,t) = u_m(x,t) + \eta_x(x,t)\phi_S^P(y,z) \tag{1a}$$

$$v(x,y,z,t) = -z\sin\theta_x(x,t) - y\big(1-\cos\theta_x(x,t)\big) \tag{1b}$$

$$w(x,y,z,t) = y\sin\theta_x(x,t) - z\big(1-\cos\theta_x(x,t)\big) \tag{1c}$$

where u, v, w are the axial and transverse bar displacement components with respect to the S_{yz} system of axes [43]; $\theta_x(x,t)$ is the angle of twist; ϕ_S^P is the primary warping function with respect to the shear center S [1]; $\eta_x(x,t)$ and $u_m(x,t)$ denote an independent warping parameter [8] and an "average" axial displacement of the bar's cross section, respectively, that will be later discussed. By dropping the displacement and rotation components related to flexure of the displacement field adopted in [2, 44], (1) are precisely recovered. Moreover, by neglecting the time variation of the defined quantities, adopting the approximations of the linear theory of torsion ($\sin\theta_x \approx \theta_x$, $\cos\theta_x \approx 1$) and having in mind that only bisymmetrical cross sections of bars under axial and torsional loading conditions are considered, the displacement field of the linear nonuniform warping beam theory can be obtained [8].

Substituting (1) in the three-dimensional nonlinear strain-displacement relations, the non-vanishing strain resultants are obtained, after neglecting the nonlinear terms of the axial displacement component [45–47], as

$$\varepsilon_{xx} = u_m' + \eta_x'\phi_S^P + \frac{1}{2}\big(y^2+z^2\big)\big(\theta_x'\big)^2 \tag{2a}$$

$$\gamma_{xy} = \eta_x\frac{\partial\phi_S^P}{\partial y} - \theta_x' z \tag{2b}$$

$$\gamma_{xz} = \eta_x\frac{\partial\phi_S^P}{\partial z} + \theta_x' y \tag{2c}$$

where the second-order geometrically nonlinear term in the right hand side of (2a) is often described as the "Wagner strain" [48]. From (2b), (2c) it is observed that shear strains are linear. However, if flexural effects were considered, both the normal and shear strains would be enriched with a series of nonlinear terms [44].

Considering strains to be small, employing the second Piola—Kirchhoff stress tensor, the Hooke's stress-strain law [5, 49] and (2), the work contributing stress components are given as

$$S_{xx} = E\left[u_m' + \eta_x'\phi_S^P + \frac{1}{2}\big(y^2+z^2\big)\big(\theta_x'\big)^2\right] \tag{3a}$$

$$S_{xy} = S_{xy}^P + S_{xy}^S \tag{3b}$$

$$\S_{xz} = S_{xz}^P + S_{xz}^S \tag{3c}$$

where

$$S_{xy}^P = G\theta_x'\left(\frac{\partial\phi_S^P}{\partial y} - z\right) \tag{4a}$$

$$S_{xz}^P = G\theta_x'\left(\frac{\partial\phi_S^P}{\partial z} + y\right) \tag{4b}$$

$$S_{xy}^S = G\big(\eta_x - \theta_x'\big)\frac{\partial\phi_S^P}{\partial y} \tag{5a}$$

$$S_{xz}^S = G\big(\eta_x - \theta_x'\big)\frac{\partial\phi_S^P}{\partial z} \tag{5b}$$

denote the well-known primary (St. Venant) shear stress distribution accounting for uniform torsion [50]

and the secondary (warping) shear stress distribution accounting for nonuniform torsion, respectively.

2.2 Primary warping function ϕ_S^P, "average" axial displacement u_m

The primary warping function is evaluated independently by exploiting local equilibrium considerations along the longitudinal x axis (after ignoring the inertia and the nonuniform torsion theory terms) from the solution of the following boundary value problem [1, 51]

$$\nabla^2 \phi_S^P = 0 \quad \text{in } \Omega \tag{6a}$$

$$\frac{\partial \phi_S^P}{\partial n} = z n_y - y n_z \quad \text{on } \Gamma_j \tag{6b}$$

where $\nabla^2 = \partial^2/\partial y^2 + \partial^2/\partial z^2$ is the Laplace operator and $\partial/\partial n$ denotes the directional derivative normal to the boundary Γ. Since the problem at hand has the Neumann type boundary condition, the evaluated warping function contains an integration constant (parallel displacement of the cross section along the bar axis), which is evaluated following the procedure presented in Sapountzakis [52]. The meaning of the "average" axial displacement of the cross section of the bar can now be explained as (1a) can be written as $\int_\Omega u \, \mathrm{d}\Omega = u_m A + \eta_x \int_\Omega \phi_S^P \, \mathrm{d}\Omega$ leading to the relation $u_m = \int_\Omega u \, \mathrm{d}\Omega / A$.

2.3 Warping shear stress distribution, independent warping parameter η_x

By substituting (1a) and (3) on the differential equation describing local equilibrium along the longitudinal axis x [35]

$$\frac{\partial S_{xx}}{\partial x} + \frac{\partial S_{xy}}{\partial y} + \frac{\partial S_{xz}}{\partial z} - \rho \ddot{u} = 0 \quad \text{in } \Omega, \forall x \in (0, l) \tag{7}$$

it is easily concluded that this equation cannot be satisfied. The same conclusion also holds for the associated boundary condition of this equation, as this is thoroughly discussed in [8] for the linear static case. Observing (5a) and (5b), it comes up that adopting the displacement field given in (1), warping shear stresses follow the distribution of the derivatives of ϕ_S^P. Moreover, a warping shear stress distribution including a secondary warping function ϕ_S^S is proved not to violate both the aforementioned equation of motion (7) and the associated boundary condition, as proposed in [3]. Therefore, employing (5) to obtain accurate values of warping shear stresses is of doubtful validity, especially near the boundary of the cross section. Nevertheless, the present formulation depending on an independent warping parameter η_x and the angle of twist θ_x, makes it possible to accurately analyze bars of either closed or open shaped cross sections. This formulation can also account for warping shear stresses in global equilibrium, which has not been achieved in previous research efforts [3] for the case of closed shaped cross sections.

2.4 Equations of motion

In order to establish the equations of motion, the principle of virtual work under a Total Lagrangian formulation is employed as this is accomplished in [35]. Performing the decomposition of shear strains into primary and secondary parts, as it is described for shear stresses in (3b), (3c), (4), (5), the contribution of shear stresses in the virtual work of internal forces can be written as

$$\begin{aligned} I_1 = \int_V \big(& S_{xy}^P \delta\gamma_{xy}^P + S_{xy}^S \delta\gamma_{xy}^S + \underline{S_{xy}^S \delta\gamma_{xy}^P} \\ & + \underline{S_{xy}^P \delta\gamma_{xy}^S} + S_{xz}^P \delta\gamma_{xz}^P + S_{xz}^S \delta\gamma_{xz}^S + \underline{S_{xz}^S \delta\gamma_{xz}^P} \\ & + \underline{S_{xz}^P \delta\gamma_{xz}^S} \big) \, \mathrm{d}V \end{aligned} \tag{8}$$

Carrying out suitable integration by parts and exploiting both (6a) and (6b), it is easily proven that the underlined terms in the above equation vanish. The remaining terms can be written more conveniently as $I_1 = \int_{x=0}^{l} [M_t^P \delta\theta_x' - M_t^S (\delta\eta_x - \delta\theta_x')] \, \mathrm{d}x$ where M_t^P, M_t^S are the primary and secondary twisting moments, respectively [1], defined here as

$$M_t^P = \int_\Omega \left[S_{xy}^P \left(\frac{\partial \phi_S^P}{\partial y} - z \right) + S_{xz}^P \left(\frac{\partial \phi_S^P}{\partial z} + y \right) \right] \mathrm{d}\Omega \tag{9a}$$

$$M_t^S = -\int_\Omega \left(S_{xy}^S \frac{\partial \phi_S^P}{\partial y} + S_{xz}^S \frac{\partial \phi_S^P}{\partial z} \right) \mathrm{d}\Omega \tag{9b}$$

Substituting (4)–(5) into (9), the above stress resultants are given (with respect to the kinematical components) as $M_t^P = G I_t \theta_x'$, $M_t^S = -G I_t^S (\eta_x - \theta_x')$ where

I_t, I_t^S are the primary (St. Venant) [52] and secondary [6] torsion constants, respectively given as

$$I_t = \int_\Omega \left(y^2 + z^2 + y\frac{\partial \phi_S^P}{\partial z} - z\frac{\partial \phi_S^P}{\partial y} \right) \mathrm{d}\Omega \tag{10a}$$

$$I_t^S = A_\theta \int_\Omega \left(-y\frac{\partial \phi_S^P}{\partial z} + z\frac{\partial \phi_S^P}{\partial y} \right) \mathrm{d}\Omega \tag{10b}$$

with A_θ defined as the "effective shear area due to the restrained torsional warping" [10]. The required algebra to reach the above expressions starting from those of (9) is presented in Appendix. Kim & Kim in [10] propose an expression to evaluate A_θ of thin-walled cross sections within the context of the stress resultants defined in this paper, while Rubin [53] presents expressions to evaluate the secondary torsion constant I_t^S of thin-walled cross sections. Numerical evaluation of A_θ of arbitrarily shaped cross sections is proposed in the recent developments of Kraus [54] employing the FEM and of Sapountzakis and Mokos [7] employing the BEM, within the context of linear static torsional loading conditions. Throughout the present work it is assumed (unless otherwise mentioned) that $A_\theta = 1$, which evidently leads to the relation $I_t = I_P - I_t^S$ with I_P denoting the polar moment of inertia. It is worth mentioning here that the above relations absolutely conform to the geometrically exact beam theory of Simo and Vu-Quok [2] and the nonuniform warping beam theory of El Fatmi [8].

It is also convenient to define the axial stress resultant N and the warping moment M_w arising from normal stresses as in [35]. Substituting the stress components given in (3), the strain ones given in (2) and the displacement ones given in (1) to the principle of virtual work, the governing partial differential equations of motion of the bar are obtained after some algebra as

$$\rho A \ddot{u}_m - EAu_m'' - EI_P \theta_x' \theta_x'' = n(x,t) \tag{11a}$$

$$\rho I_p \ddot{\theta}_x - G\left(I_t + I_t^S\right)\theta_x'' + GI_t^S \eta_x' - \frac{3}{2} EI_{PP}\left(\theta_x'\right)\theta_x'' - EI_p u_m' \theta_x'' - EI_p u_m'' \theta_x' = m_t(x,t) \tag{11b}$$

$$\rho C_S \ddot{\eta}_x - EC_S \eta_x'' + GI_t^S\left(\eta_x - \theta_x'\right) = -m_w(x,t) \tag{11c}$$

subjected to the initial conditions ($x \in (0, l)$)

$$u_m(x,0) = \bar{u}_{m0}(x) \tag{12a}$$

$$\dot{u}_m(x,0) = \dot{\bar{u}}_{m0}(x) \tag{12b}$$

$$\theta_x(x,0) = \bar{\theta}_{x0}(x) \tag{12c}$$

$$\dot{\theta}_x(x,0) = \dot{\bar{\theta}}_{x0}(x) \tag{12d}$$

$$\eta_x(x,0) = \bar{\eta}_{x0}(x) \tag{12e}$$

$$\dot{\eta}_x(x,0) = \dot{\bar{\eta}}_{x0}(x) \tag{12f}$$

together with the boundary conditions at the bar ends $x = 0, l$

$$\alpha_1 N + \alpha_2 u_m = \alpha_3 \tag{13a}$$

$$\beta_1 M_t + \beta_2 \theta_x = \beta_3 \tag{13b}$$

$$\bar{\beta}_1 M_w + \bar{\beta}_2 \eta_x = \bar{\beta}_3 \tag{13c}$$

where N, M_t, M_w are the axial force, twisting and warping moments at the bar ends, respectively given as

$$N = EAu_m' + \frac{1}{2} EI_P\left(\theta_x'\right)^2 \tag{14a}$$

$$M_t = G\left(I_t + I_t^S\right)\theta_x' - GI_t^S \eta_x + EI_P u_m' \theta_x' + \frac{1}{2} EI_{PP}\left(\theta_x'\right)^3 \tag{14b}$$

$$M_w = -EC_S \eta_x' \tag{14c}$$

while α_i, β_i, $\bar{\beta}_i$ $(i = 1, 2, 3)$ are time dependent functions specified at the boundary of the bar. The geometric constants I_{PP}, C_S appearing in (11) and (14) are given in [35], while the externally applied loads are related to the components of the traction vector with respect to the undeformed surface of the bar t_x, t_y, t_z as

$$n(x,t) = \int_\Gamma t_x \,\mathrm{d}s \tag{15a}$$

$$m_t(x,t) = \int_\Gamma t_y(-z\cos\theta_x - y\sin\theta_x) + t_z(y\cos\theta_x - z\sin\theta_x)\,\mathrm{d}s \tag{15b}$$

$$m_w(x,t) = -\int_\Gamma t_x \phi_S^P \,\mathrm{d}s \tag{15c}$$

The boundary conditions (13) are the most general boundary conditions for the problem at hand, including also the elastic support. It is worth here noting that the terms of the boundary conditions of (13) are nonlinear by virtue of (14), while linear viscous damping could also be included in (11) without any special difficulty. Moreover, from (11) it is concluded that all of

the inertia terms are linear. However, if flexural effects were considered, nonlinear inertia terms would arise in the governing equations as well [44].

It is worth here noting that all the relations established so far are completely analogous to those of the Timoshenko beam theory, modeling the shear—bending loading conditions of bars. The analogy of all the kinematical and stress components with the ones of the Timoshenko beam theory is thoroughly presented in [6] for the linear static case.

The established initial boundary value problem is a coupled and nonlinear one. A significant reduction on the set of differential equations can be achieved by neglecting the axial inertia term $\rho A\ddot{u}_m$ of (11a), a common assumption among dynamic beam formulations. Ignoring this term, two partial differential equations with respect to two unknown displacement components $(\theta_x(x,t), \eta_x(x,t))$ can be obtained. These equations can be further combined by performing similar algebraic manipulations as the ones described in [55–58] so as to formulate a single partial differential equation with respect to $\theta_x(x,t)$. This equation can then be directly compared with the corresponding one presented in [35] that does not account for secondary twisting moment deformation effect (STMDE). In what follows, these procedures are described in detail for the case of constant along the bar axial load which is of great practical interest, especially in torsional postbuckling analysis of bars.

2.5 Reduced initial boundary value problem for constant along the bar axial load

For the case of constant along the bar axial load, the axial boundary conditions (13a) are written as

$$u_m(0,t) = 0 \tag{16a}$$

$$N(l,t) = \bar{N}(l,t) \tag{16b}$$

Employing the aforementioned simplifications, (11a) gives $u_m'' = -\frac{I_P}{A}\theta_x'\theta_x''$, $\forall x \in (0,l)$ which after subsequent integration and utilization of (16) yields $u_m' = -\frac{1}{2}\frac{I_P}{A}(\theta_x')^2 + \frac{\bar{N}}{EA}$, $\forall x \in [0,l]$. Substituting the expressions of u_m'', u_m' into (11b), (14b) the reduced initial boundary value problem is established as

$$\rho I_P\ddot{\theta}_x - \left(GI_t + GI_t^S + \frac{I_P}{A}\bar{N}\right)\theta_x'' + GI_t^S\eta_x' - \frac{3}{2}EI_n(\theta_x')^2\theta_x'' = m_t(x,t) \tag{17}$$

along with the governing (11c), the pertinent initial conditions (12c), (12d), (12e), (12f) and boundary conditions (13b), (13c). It is worth here noting that (14a), (14c) hold, whereas (14b) is modified as

$$M_t = \left(GI_t + GI_t^S + \frac{I_P}{A}\bar{N}\right)\theta_x' - GI_t^S\eta_x + \frac{1}{2}EI_n(\theta_x')^3 \tag{18}$$

where I_n is a nonnegative geometric cross sectional property related to the geometrical nonlinearity expressed as $I_n = I_{PP} - \frac{I_P^2}{A}$.

The equations of motion (17), (11c) can be further combined by performing similar algebraic manipulations with those presented in [55–57] leading the initial boundary value problem to a single partial differential equation with respect to $\theta_x(x,t)$. More specifically, (17) is solved with respect to η_x' and the obtained expression is substituted in the differentiated with respect to x version of (11c), resulting the following governing partial differential equation with respect to the angle of twist as

$$\begin{aligned}
&\rho I_P\ddot{\theta}_x - \rho C_S\left(\frac{1}{\kappa} + \frac{EI_P}{GI_t^S} + \frac{I_P}{GI_t^S A}\bar{N}\right)\ddot{\theta}_x'' \\
&- \rho C_S\frac{EI_n}{GI_t^S}\left[3(\dot{\theta}_x')^2\theta_x'' + 6\dot{\theta}_x'\dot{\theta}_x''\theta_x' + 3\ddot{\theta}_x'\theta_x'\theta_x'' + 3\ddot{\theta}_x'(\theta_x')^2\right] + EC_S\left(\frac{1}{\kappa} + \frac{I_P}{GI_t^S A}\bar{N}\right)\theta_x'''' \\
&- \left(GI_t + \frac{I_P}{A}\bar{N}\right)\theta_x'' - \frac{3}{2}EI_n(\theta_x')^2\theta_x'' \\
&+ EI_n\frac{EC_S}{GI_t^S}\left[3(\theta_x'')^3 + 9\theta_x'\theta_x''\theta_x''' + \frac{3}{2}(\theta_x')^2\theta_x''''\right] \\
&= m_t + m_w' + \frac{\rho C_S}{GI_t^S}\ddot{m}_t - \frac{EC_S}{GI_t^S}m_t''
\end{aligned} \tag{19}$$

after neglecting the higher order term $\rho C_S[\rho I_P/(GI_t^S)]\ddot{\theta}_x''$. Equation (19) must satisfy the pertinent initial conditions (12c), (12d) and boundary conditions

(13b), (13c), where the independent warping parameter η_x and the twisting and warping moments M_t, M_w are given (at the bar ends $x = 0, l$) as

$$\eta_x = \theta_x' + \frac{EC_S}{GI_t^S}\left(\frac{1}{\kappa} + \frac{I_P}{GI_t^S A}\bar{N}\right)\theta_x''' + \frac{EC_S}{GI_t^S}\frac{EI_n}{GI_t^S}\left[3\theta_x'\left(\theta_x''\right)^2 + \frac{3}{2}\left(\theta_x'\right)^2\theta_x'''\right] \tag{20a}$$

$$M_t = \left(GI_t + \frac{I_P}{A}\bar{N}\right)\theta_x' - EC_S\left(\frac{1}{\kappa} + \frac{I_P}{GI_t^S A}\bar{N}\right)\theta_x''' + \frac{1}{2}EI_n\left(\theta_x'\right)^3 - EC_S\frac{EI_n}{GI_t^S}\left[3\theta_x'\left(\theta_x''\right)^2 + \frac{3}{2}\left(\theta_x'\right)^2\theta_x'''\right] \tag{20b}$$

$$M_w = EC_S\left(\frac{1}{\kappa} + \frac{I_P}{GI_t^S A}\bar{N}\right)\theta_x'' + EC_S\frac{EI_n}{GI_t^S}\left[\frac{3}{2}\left(\theta_x'\right)^2\theta_x''\right] \tag{20c}$$

In the above equations κ is an auxiliary geometric constant related to the secondary twisting moment deformation effect given as $\kappa = I_t^S/(I_t + I_t^S)$.

Comparing the formulated reduced initial boundary value problem and the one presented in [35] where the STMDE is not taken into account, it is concluded that this effect alters the expressions of warping inertia, warping stiffness and external loading and induces higher order nonlinear inertia and stiffness terms in the governing partial differential equation. Some nonlinear stiffness terms are also induced in the kinematical and stress components at the bar ends. If the STMDE is neglected, the displacement field (1) must be updated by substituting $\eta_x = \theta_x'$ (and all the subsequent equations accordingly) as well as (19)–(20) by substituting $\kappa = 1$ and dropping all the terms related to I_t^S.

3 Integral representations—numerical solution

3.1 For the angle of twist θ_x

According to the precedent analysis, the nonlinear nonuniform torsional vibration problem of shear deformable bars reduces to establishing the displacement component $\theta_x(x,t)$ having continuous partial derivatives up to the fourth order with respect to x and up to the second order with respect to t, satisfying the nonlinear initial boundary value problem described by the partial differential equation (19), the initial conditions (12c), (12d) along the bar and the boundary conditions (13b), (13c) at the bar ends $x = 0, l$. This problem is solved using the Analog Equation Method [42]. Employing this method as this is presented in [35] and applying (19) to L collocation points, L semidiscretized nonlinear equations of motion are formulated as

$$\mathbf{M}\{\ddot{\mathbf{d}}\} + \mathbf{K}\{\mathbf{d}\} + \mathbf{m}^{nl}(\mathbf{H}_1, \mathbf{H}_2, \dot{\mathbf{d}}, \ddot{\mathbf{d}}) + \mathbf{k}^{nl}(\mathbf{H}_1, \mathbf{H}_2, \mathbf{H}_3, \mathbf{d}) = \mathbf{f} \tag{21}$$

where $\mathbf{d}$ is a $L + 8$ generalized unknown vector, $\mathbf{m}^{nl}, \mathbf{k}^{nl}$ are nonlinear generalized mass vector and stiffness vector respectively and $\mathbf{M}$, $\mathbf{K}$, $\mathbf{f}$ are generalized mass matrix, stiffness matrix and force vector respectively, given as

$$\left\{\mathbf{m}^{nl}\right\}_i = -\rho C_S\frac{EI_n}{GI_t^S}\Big[3\big[\{\mathbf{H}_1\}_i\dot{\mathbf{d}}\big]^2\big(\{\mathbf{H}_2\}_i\mathbf{d}\big) + 6\big(\{\mathbf{H}_1\}_i\dot{\mathbf{d}}\big)\big(\{\mathbf{H}_2\}_i\dot{\mathbf{d}}\big)\big(\{\mathbf{H}_1\}_i\mathbf{d}\big) + 3\big(\{\mathbf{H}_1\}_i\ddot{\mathbf{d}}\big)\big(\{\mathbf{H}_1\}_i\mathbf{d}\big)\big(\{\mathbf{H}_2\}_i\mathbf{d}\big) + 3\big(\{\mathbf{H}_1\}_i\ddot{\mathbf{d}}\big)\big[\{\mathbf{H}_1\}_i\mathbf{d}\big]^2\Big] \tag{22a}$$

$$\left\{\mathbf{k}^{nl}\right\}_i = -\frac{3}{2}EI_n\big[\{\mathbf{H}_1\}_i\mathbf{d}\big]^2\big(\{\mathbf{H}_2\}_i\mathbf{d}\big) + EI_n\frac{EC_S}{GI_t^S}\Big[3\big[\{\mathbf{H}_2\}_i\mathbf{d}\big]^3 + 9\big(\{\mathbf{H}_1\}_i\mathbf{d}\big)\big(\{\mathbf{H}_2\}_i\mathbf{d}\big)\big(\{\mathbf{H}_3\}_i\mathbf{d}\big) + \frac{3}{2}\big[\{\mathbf{H}_1\}_i\mathbf{d}\big]^2\{\mathbf{d}\}_i\Big] \tag{22b}$$

$$\mathbf{M} = \left[\rho I_P\mathbf{H}_0 - \rho C_S\left(\frac{1}{\kappa} + \frac{EI_P}{GI_t^S} + \frac{I_P}{GI_t^S A}\bar{N}\right)\mathbf{H}_2\right] \tag{22c}$$

$$\mathbf{K} = \left[-\left(GI_t + \frac{I_P}{A}\bar{N}\right)\mathbf{H}_2 + EC_S\left(\frac{1}{\kappa} + \frac{I_P}{GI_t^S A}\bar{N}\right)\mathbf{I0}\right] \tag{22d}$$

$$\mathbf{f} = \left\{\mathbf{m_t} + \mathbf{m_w'} + \frac{\rho C_S}{GI_t^S}\ddot{\mathbf{m}}_\mathbf{t} - \frac{EC_S}{GI_t^S}\mathbf{m_t''}\right\} \tag{22e}$$

In the above equations, $\{\cdot\}_i$ denotes the (arbitrary) ith row ($i = 1, 2, \ldots, L$) of the matrix inside the brackets,

$\mathbf{H}_j (j = 0, 1, 2, 3)$ are $L \times (L+8)$ known matrices, $\mathbf{I0}$ is an $L \times (L+8)$ rectangular matrix given as $\mathbf{I0} = [\mathbf{I}\ \mathbf{0}]$ with $\mathbf{I}$ and $\mathbf{0}$ being the $L \times L$ identity matrix and the $L \times 8$ rectangular matrix with zero elements, respectively, while $\mathbf{m_t}, \mathbf{m'_w}, \ddot{\mathbf{m}}_\mathbf{t}, \mathbf{m''_t}$ are vectors containing the values of the dynamic external loading at the L nodal points. The elements of $\mathbf{m'_w}, \mathbf{m''_t}$ can be written with respect to the values of $m_w(x,t), m_t(x,t)$, respectively at the collocation points by using appropriate finite differences [59]. Equation (21) along with 8 algebraic equations constitute a system of simultaneous $L + 8$ Differential—Algebraic equations (DAE). The details of the derivation as well as the solution algorithm of this system of equations can be retrieved in [35].

3.2 For the primary warping function ϕ_S^P

The integral representations and the numerical solution for the evaluation of the angle of twist θ_x presented in the previous section assume that the warping C_S and the torsion I_t, I_t^S constants are already established. The expressions of these constants indicate that their evaluation presumes that ϕ_S^P at any interior point of the domain Ω of the cross section of the bar is known. Once ϕ_S^P is established, C_S and I_t constants are evaluated by converting the domain integrals into line integrals along the boundary using the corresponding relations presented in Sapountzakis and Mokos [1], while the line integral expression of I_t^S constant is written as $I_t^S = \int_\Gamma \phi_S^P (z n_y - y n_z)\, \mathrm{d}s$.

4 Numerical examples

On the basis of the analytical and numerical procedures presented in the previous sections, a computer program has been written and representative examples have been studied to demonstrate the validation, efficiency and the range of applications of the developed method. It is noted that the probability of the bar's exhibiting chaotic motion in its nonlinear response is not investigated within the present study.

Example 1 (Small amplitude free vibrations, open shaped cross section) In the first three examples, an open thin-walled I-shaped cross section bar ($E = 2.1 \times 10^8$ kN/m^2, $G = 8.1 \times 10^7$ kN/m^2, $\rho = 8.002$ kN s^2/m^4) of length $l = 4.0$ m, having flange and web width $t_f = t_w = 0.01$ m, total height and total width $h = b = 0.20$ m has been studied, while the numerical results have been obtained employing 21 nodal points (longitudinal discretization) and 400 boundary elements (cross section discretization). The geometric constants of the bar are computed as $A = 5.800 \times 10^{-3}$ m^2, $I_P = 5.434 \times 10^{-5}$ m^4, $I_n = 1.631 \times 10^{-7}$ m^6, $I_{PP} = 6.722 \times 10^{-7}$ m^6, $I_t = 2.080 \times 10^{-7}$ m^4, $I_t^S = 5.413 \times 10^{-4}$ m^4, $C_S = 1.200 \times 10^{-7}$ m^6. The bar's ends are simply supported according to its torsional boundary conditions, while the left end is immovable and the right end is subjected to a compressive axial load according to its axial boundary conditions.

In the first example, for comparison reasons, the axial load—torsional fundamental natural frequency relation of the aforementioned bar has been investigated. Mohri et al. [41], without considering the secondary twisting moment deformation effect, proposed analytical load—frequency relations by dropping the higher order warping inertia term and assuming that (i) the fundamental modeshape of vibration follows a sinusoidal form $\sin(\frac{\pi x}{l})$ both in the pre- and postbuckling region, (ii) the bar vibrates harmonically, (iii) vibrations of small amplitude around a static equilibrium state are performed. These load ($\bar{N}$)—frequency (ω_f) relations for the pre- and postbuckling regions are given, respectively, as

$$\omega_f^2 = \omega_\theta^2 \left(1 - \frac{\bar{N}}{\bar{N}_{cr,\theta}}\right) \tag{23a}$$

$$\omega_f^2 = 2\omega_\theta^2 \left(\frac{\bar{N}}{\bar{N}_{cr,\theta}} - 1\right) \tag{23b}$$

where ω_θ is the natural frequency for vanishing axial load and $\bar{N}_{cr,\theta}$ is the torsional buckling load of the bar, respectively given as [41]

$$\omega_\theta^2 = \frac{\pi^2}{\rho l^2 I_P} \left(\frac{\pi^2 E C_S}{l^2} + G I_t\right) \tag{24a}$$

$$\bar{N}_{cr,\theta} = \frac{A}{I_P} \left(\frac{\pi^2 E C_S}{l^2} + G I_t\right) \tag{24b}$$

According to our results, the nonlinear initial boundary value problem ((19), (12c), (12d), (13b), (13c)) has been solved for several values of constant axial load $\bar{N}$ to obtain the response of the bar in the time domain, taking into account or neglecting the

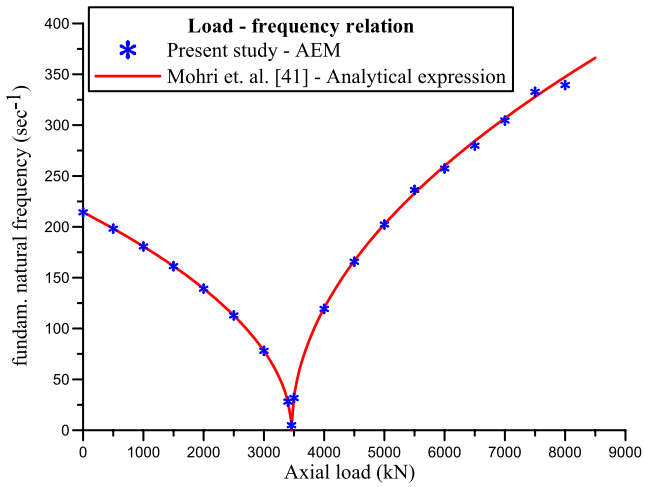

Fig. 2 Axial load $\bar{N}$—torsional fundamental natural frequency ω_f relation of (23) [41] along with pairs of values $(\omega_f, \bar{N})$ obtained from present study (Example 1)

STMDE. The fundamental natural frequency ω_f is then computed by exploiting the first few full cycles of vibration. The computation is based on the Fast Fourier Transform (FFT) of the time history, while a Hanning data window is employed [60]. The free vibrations are initiated by dropping all the torsional loading terms and by employing the linear fundamental modeshape of the angle of twist as initial twisting rotations $\bar{\theta}_{x0}(x)$ [35] along with zero initial twisting velocities $\dot{\bar{\theta}}_{x0}(x)$. In all cases, the STMDE is neglected in the evaluation of $\bar{\theta}_{x0}(x)$. $\bar{\theta}_{x0}(x)$ is computed by employing the methodology presented in [35] and corresponds to the sinusoidal form assumed by Mohri et al. [41]. In order to perform vibrations of small amplitude, the initial midpoint angle of twist amplitude $\bar{\theta}_{x0}(l/2)$ is chosen closely to the midpoint angle of twist amplitude $\theta_0(l/2)$ corresponding to the static equilibrium state. Mohri et al. [41, 61] assuming that the twisting deformation mode follows a sinusoidal form $\sin(\frac{\pi x}{l})$ proposed the following analytical expression to evaluate $\theta_0(l/2)$

$$\theta_0(l/2) = \begin{cases} 0, & \text{prebuckling region} \\ \pm\sqrt{\frac{8l^2}{3\pi^2}\frac{I_P}{EAI_n}(\bar{N} - \bar{N}_{cr,\theta})}, & \text{postbuckling region} \end{cases} \tag{25}$$

In Fig. 2, the load–frequency relations of (23) are presented along with pairs of values $(\omega_f, \bar{N})$ obtained from the proposed method, ignoring the STMDE. The pairs $(\omega_f, \bar{N})$ are computed by using the values of initial midpoint angle of twist amplitude $\bar{\theta}_{x0}(l/2)$, which are given in Table 1 along with the corresponding values of $\theta_0(l/2)$ computed from (25). From Fig. 2, the validity of the proposed method in predicting $\bar{N}$–ω_f pairs of values of bars undergoing small amplitude torsional vibrations is concluded. The higher discrepancies between the two sets of solutions in the postbuckling region as compared to the ones in the prebuckling region are attributed to the fact that the previously mentioned assumptions (i), (ii) are valid only in the prebuckling region. To illustrate this point better, in Figs. 3a, b the obtained time histories of the angle of twist $\theta_x(l/2, t)$ at the midpoint of the bar for a prebuckling ($\bar{N} = -1000$ kN) and a postbuckling ($\bar{N} = -5000$ kN) axial loading are presented, respectively, demonstrating that only the buckled bar undergoes multifrequency vibrations. For comparison pur-

Table 1 Axial load $\bar{N}$, midpoint angle of twist amplitude $\theta_0(l/2)$ corresponding to the static equilibrium state [41], along with values of initial midpoint angle of twist amplitude $\bar{\theta}_{x0}(l/2)$ used to initiate free vibrations of Example 1

$\lvert\bar{N}\rvert$ (kN)	$\theta_0(l/2)$ (rad)	$\bar{\theta}_{x0}(l/2)$ (rad)
0–3458	0.00	0.05
3500	0.22	0.27
4000	0.80	0.85
4500	1.11	1.16
5000	1.35	1.40
5500	1.55	1.60
6000	1.73	1.85
6500	1.90	2.00
7000	2.05	2.20
7500	2.19	2.35
8000	2.32	2.50

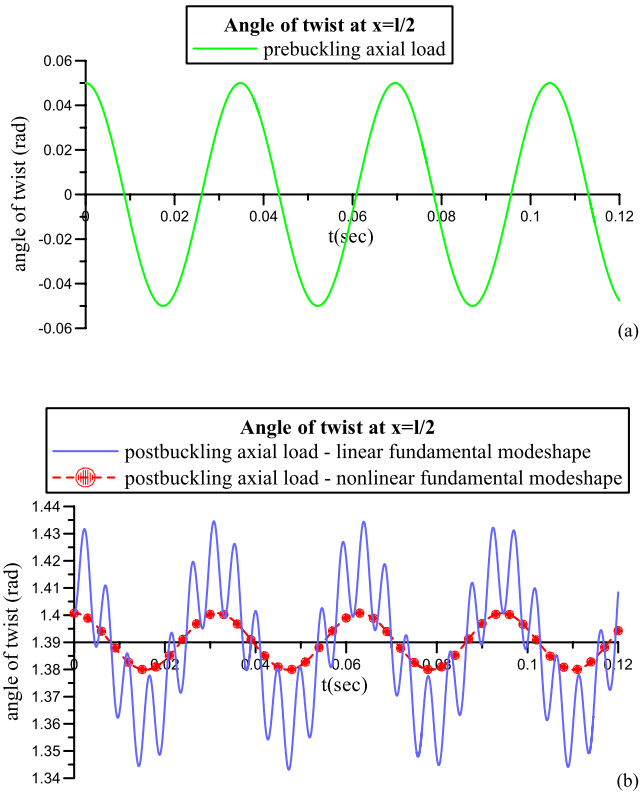

Fig. 3 Time histories of the angle of twist at the midpoint of the bar of Example 1, for a prebuckling ($\bar{N} = -1000$ kN) (**a**) and a postbuckling ($\bar{N} = -5000$ kN) (**b**) axial loading

Table 2 Pairs of values $\bar{N}$(kN)–ω_f(s^{-1}) taking into account or ignoring the STMDE and employing the linear or the nonlinear fundamental modeshape as initial twisting rotations $\bar{\theta}_{x0}(x)$ for the free vibrations of Example 1

$\lvert\bar{N}\rvert$ (kN)	ω_f (s^{-1})			
	$\bar{\theta}_{x0}(x)$: linear fundamental modeshape		$\bar{\theta}_{x0}(x)$: nonlinear fundamental modeshape	
	With STMDE	Without STMDE	With STMDE	Without STMDE
1000	180.48	180.70	–	–
5000	199.77	199.46	199.98	199.67

poses, in Fig. 3b the time history of $\theta_x(l/2, t)$ employing the nonlinear fundamental modeshape of the angle of twist as initial twisting rotations $\bar{\theta}_{x0}(x)$ (along with zero initial twisting velocities $\dot{\bar{\theta}}_{x0}(x)$) is also included ($\bar{N} = -5000$ kN), showing that the initiation of free vibrations with the nonlinear modeshape does not induce higher harmonics in the response of the bar. Finally, in Table 2 the obtained results of pairs of values $(\omega_f, \bar{N})$ are presented taking into account or ignoring the STMDE and employing either the linear or the nonlinear fundamental modeshape to initiate the free vibrations, showing that in both pre- and post- buckling regions, the STMDE does not affect the fundamental natural frequency of bars of open thin-walled cross sections undergoing small amplitude vibrations. The insignificance of the STMDE for linear static loading conditions of bars of such cross sections has already been reported in the literature [6].

Example 2 (Nonlinear free vibrations, open shaped cross section) In the second example, the effect of geometrical nonlinearity on the dynamic characteristics of the bar under examination (bar of Example 1) at a postbuckled state is investigated. The nonlinear initial boundary value problem ((19), (12c), (12d), (13b), (13c)) has been solved for $\bar{N} = -5500$ kN ($|\bar{N}| > |\bar{N}_{cr,\theta}|$) for several values of initial midpoint angle of

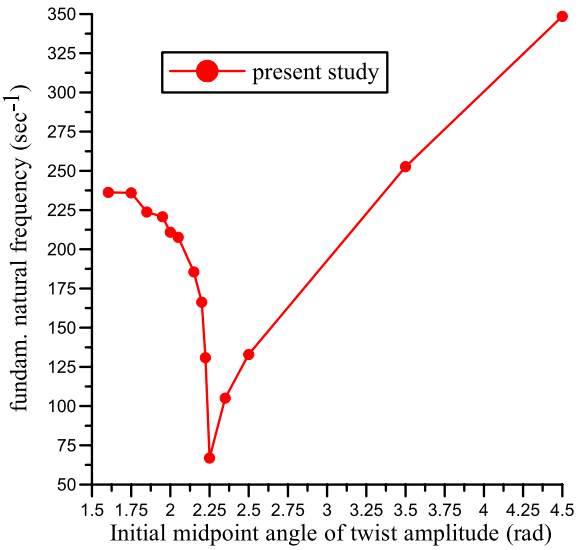

Fig. 4 Variation of the torsional fundamental natural frequency ω_f with respect to the initial midpoint angle of twist amplitude $\bar{\theta}_{x0}(l/2)$ of the bar of Example 2 ($\bar{N} = -5500$ kN)

Table 3 Initial midpoint angle of twist amplitudes $\bar{\theta}_{x0}(l/2)$ and positions $\bar{\theta}_{x,m}(l/2)$ around which vibrations are performed of the free vibrating bar of Example 2 ($\bar{N} = -5500$ kN)

$\bar{\theta}_{x0}(l/2)$ (rad)	$\bar{\theta}_{x,m}(l/2)$ (rad)
1.60	1.60
1.75	1.60
1.85	1.58
1.95	1.55
2.00	1.53
2.05	1.50
2.15	1.41
2.20	1.34
2.22	1.23
2.25	0.00
2.35	0.00
2.50	0.00
3.50	0.00
4.50	0.00

twist amplitude $\bar{\theta}_{x0}(l/2)$ to obtain the response of the bar in the time domain, taking into account or ignoring the STMDE. The free vibrations are initiated by dropping all the torsional loading terms and by considering the linear fundamental modeshape of the angle of twist as initial twisting rotations $\bar{\theta}_{x0}(x)$ along with zero initial twisting velocities $\dot{\bar{\theta}}_{x0}(x)$. In all cases, $\bar{\theta}_{x0}(x)$ is evaluated numerically ignoring the STMDE [35]. The fundamental natural frequency ω_f and the position around which vibrations are performed are then computed by exploiting the first few full cycles of vibration.

In Fig. 4, the variation of the torsional fundamental natural frequency ω_f with respect to the initial midpoint angle of twist amplitude $\bar{\theta}_{x0}(l/2)$ of the bar is presented for a range of values of $\bar{\theta}_{x0}(l/2)$, while in Table 3 the positions $\bar{\theta}_{x,m}(l/2)$ around which vibrations are performed are given for several values of $\bar{\theta}_{x0}(l/2)$. It is concluded that the geometrical nonlinearity has a profound effect on both the natural frequency of the bar and the positions around which vibrations are performed. From Table 3, it is observed that these positions are non-constant ones and depend on the initial amplitude of vibration, while for large values of $\bar{\theta}_{x0}(l/2)$ they coincide with the static equilibrium position of the prebuckling region. From Fig. 4 it is also concluded that the $\bar{\theta}_{x0}(l/2) - \omega_f$ relation is rather complex and differs significantly from the one of the prebuckling region. In the pre-buckled state, the increase of initial amplitude of vibration always leads to an increase of the bar's stiffness and eventually an increase of ω_f (see also [35], and [34] for the case of axially immovable ends and $I_n = 0$).

In Figs. 5, 6 the time histories of the angle of twist $\theta_x(l/2, t)$ at the midpoint of the bar and of the axial displacement $u_m(l, t)$ at the bar's right end, respectively, for two cases of the initial midpoint angle of twist amplitude ($\bar{\theta}_{x0}(l/2) = 2.20$ rad, $\bar{\theta}_{x0}(l/2) = 2.50$ rad) are presented taking into account or ignoring the STMDE. From these figures it is verified that especially for the case of $\bar{\theta}_{x0}(l/2) = 2.50$ rad, the frequency of the axial displacement's response is twice as much as the one of the twisting rotation's one. This effect has already been documented in the literature for nonlinear torsional vibrations of bars at prebuckling configurations [35] and nonlinear flexural vibrations of bars at prebuckling configurations with axially immovable ends [62]. Apparently, this is no longer valid when vibrations at postbuckling configurations are performed around positions with $\bar{\theta}_{x,m}(l/2)(\text{rad}) \neq 0$ (case of $\bar{\theta}_{x0}(l/2) = 2.20$ rad). From Figs. 5, 6, it is also observed that the STMDE does not influence the kinematical components of buckled bars of open thin-walled cross sections, undergoing large amplitude vibrations. This conclusion does not depend on the magnitude of the initial midpoint angle of twist amplitude.

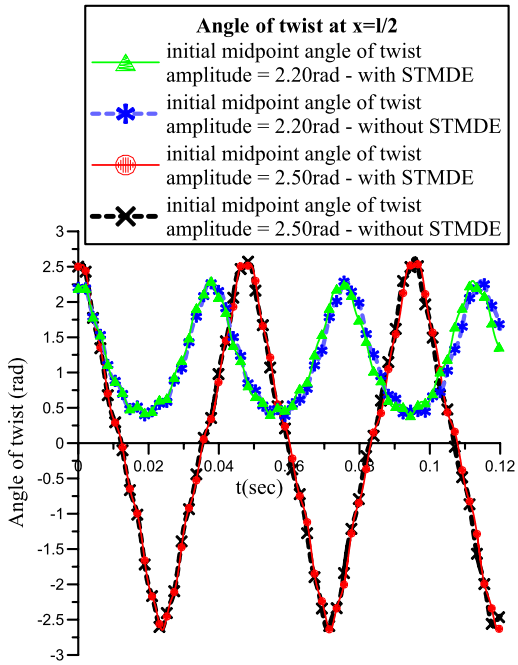

Fig. 5 Time histories of the angle of twist at the midpoint of the free vibrating bar of Example 2 taking into account or ignoring the secondary twisting moment deformation effect ($\bar{\theta}_{x0}(l/2) = 2.20$ rad, $\bar{\theta}_{x0}(l/2) = 2.50$ rad)

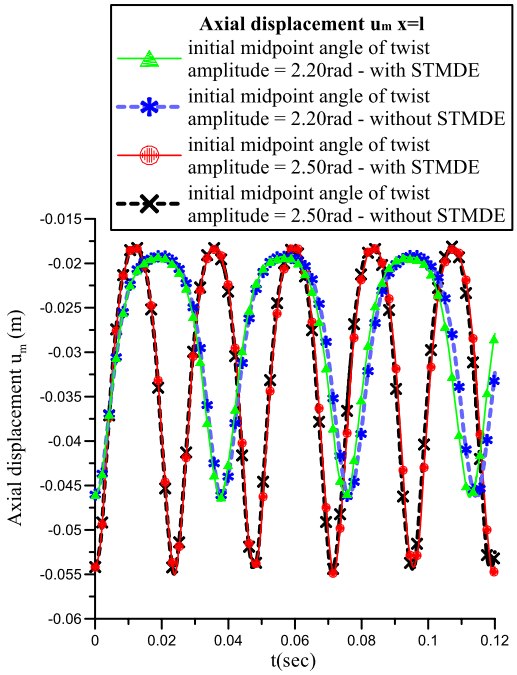

Fig. 6 Time histories of the axial displacement at the bar's right end of the free vibrating bar of Example 2 taking into account or ignoring the secondary twisting moment deformation effect ($\bar{\theta}_{x0}(l/2) = 2.20$ rad, $\bar{\theta}_{x0}(l/2) = 2.50$ rad)

In Figs. 7, 8, the time histories of the primary twisting moment M_t^P (first two terms of (20b) including the twisting moment caused by the axial load $\bar{N}$), the linear secondary twisting moment $M_{t,\text{lin}}^S$ (third and fourth terms of (20b)), the nonlinear twisting moment $M_{t,\text{nl}}$ (rest nonlinear terms of (20b)) and the total twisting moment $M_t = M_t^P + M_{t,\text{lin}}^S + M_{t,\text{nl}}$ at the bar's left end are presented taking into account the STMDE for two cases of the initial midpoint angle of twist amplitude ($\bar{\theta}_{x0}(l/2) = 2.20$ rad, $\bar{\theta}_{x0}(l/2) = 2.50$ rad), respectively. Finally, in Table 4 the extreme values of the kinematical and stress components depicted in Figs. 5, 6, 7, and 8, obtained for the time interval $0.00 \leq t \leq 0.12$ (s) are presented taking into account or ignoring the STMDE, for $\bar{\theta}_{x0}(l/2) = 2.20$ rad. From this table it is deduced that the STMDE influences negligibly both kinematical and stress components of buckled bars of open thin-walled cross sections undergoing large amplitude vibrations.

Example 3 (Primary resonance, geometrical nonlinearity, open shaped cross section) In the third example, the forced vibrations of the bar under examination (bar of Example 1) at a pre-buckled state ($\bar{N} = 0$) are investigated to determine the effects of geometrical nonlinearity and secondary twisting moment deformation. More specifically, the primary resonance of the bar is studied by applying a concentrated twisting moment $M_{t,\text{ext}}$ at its midpoint given as $M_{t,\text{ext}}(t) = M_{t0}\sin(\omega_{f,\text{lin}}t)$, where $M_{t0} = 5$ kN m and $\omega_{f,\text{lin}} = 214.23$ s^{-1} (initial conditions $\bar{\theta}_{x0}(x) = 0, \dot{\bar{\theta}}_{x0}(x) = 0$). $\omega_{f,\text{lin}}$ is the fundamental natural frequency of the bar undergoing linear torsional vibrations, ignoring STMDE and is numerically evaluated by performing modal analysis as this is presented in [63].

In Figs. 9, 10, the time histories of the angle of twist $\theta_x(l/2, t)$ at the midpoint of the bar are presented (with or without STMDE) for two cases of analysis, namely ignoring or considering geometrical nonlinearity, respectively. The linear analyses are carried out by dropping all the nonlinear terms of (19), (20). As expected, only in the linear cases (Fig. 9) deformations continue to increase with time. The beating phenomenon observed in the nonlinear response (Fig. 10) is explained from the fact that large twisting rotations increase the bar's fundamental natural frequency ω_f (by increasing the stiffness of the bar), thereby caus-

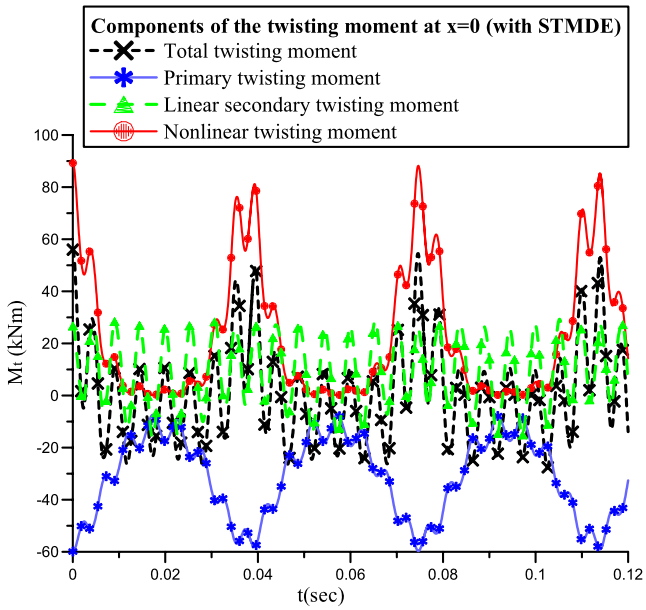

Fig. 7 Time histories of various twisting moment components at the left end of the free vibrating bar of Example 2 taking into account the secondary twisting moment deformation effect for initial midpoint angle of twist amplitude $\bar{\theta}_{x0}(l/2) = 2.20$ rad

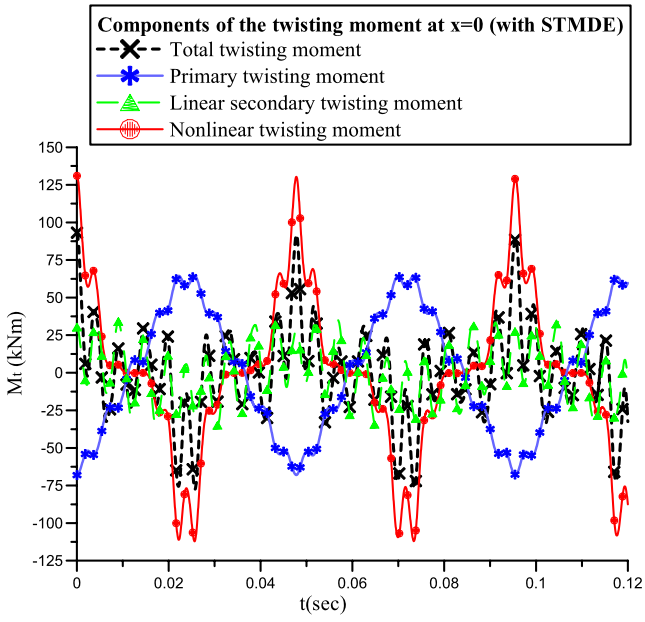

Fig. 8 Time histories of various twisting moment components at the left end of the free vibrating bar of Example 2 taking into account the secondary twisting moment deformation effect for initial midpoint angle of twist amplitude $\bar{\theta}_{x0}(l/2) = 2.50$ rad

ing a detuning of ω_f with the frequency of the external loading ($\omega_{f,\text{lin}}$). After the angle of twist reaches its maximum value, the amplitude of twisting deformations decreases, leading to the reversal of the previously mentioned effects. Moreover, in Fig. 11, the time histories of the primary twisting moment M_t^P (first two terms of (20b)), the linear secondary twisting moment $M_{t,\text{lin}}^S$ (third and fourth terms of (20b)), the nonlinear twisting moment $M_{t,\text{nl}}$ (rest nonlinear terms of (20b)) and the total twisting moment $M_t = M_t^P + M_{t,\text{lin}}^S + M_{t,\text{nl}}$ at the bar's left end are presented taking into account the STMDE and performing geometrically nonlinear analysis. Finally, in Table 5 the extreme values of the kinematical and stress components depicted in Figs. 10, 11, obtained for the time interval $0.00 \leq t \leq 0.30$ (s) are presented taking into account or ignoring the STMDE. From Fig. 10 and from Table 5 it is deduced that the STMDE influences neg-

Table 4 Extreme values of various kinematical and stress components of the free vibrating bar of Example 2, obtained for $0.00 \le t \le 0.12$ (s) ($\bar{\theta}_{x0}(l/2) = 2.20$ rad)

	With STMDE	Without STMDE
$\max \theta_x(l/2)$ (rad)	2.307	2.304
$\min \theta_x(l/2)$ (rad)	0.393	0.373
$\max u_m(l)$ (m)	−0.019	−0.019
$\min u_m(l)$ (m)	−0.046	−0.046
$\max M_t^P(0)$ (kN m)	−7.178	−6.796
$\min M_t^P(0)$ (kN m)	−59.927	−59.927
$\max M_{t.\mathrm{lin}}^S(0)$ (kN m)	29.277	28.775
$\min M_{t.\mathrm{lin}}^S(0)$ (kN m)	−16.208	−15.697
$\max M_{t.\mathrm{nl}}(0)$ (kN m)	89.261	88.321
$\min M_{t.\mathrm{nl}}(0)$ (kN m)	0.144	0.129
$\max M_t(0)$ (kN m)	55.993	55.266
$\min M_t(0)$ (kN m)	−27.665	−26.828

ligibly both kinematical and stress components of bars of open thin-walled cross sections undergoing forced vibrations.

Example 4 (Linear forced vibrations, closed shaped cross section)

In the last example, the (geometrically) linear response of a bar ($E = 2.1 \times 10^8$ kN/m^2, $G = 8.1 \times 10^7$ kN/m^2, $\rho = 8.002$ kN s^2/m^4, $l = 5.0$ m) of a closed box-shaped cross section is studied. The cross section is of total height $h = 1.64$ m, total width $b = 1.05$ m, horizontal walls thickness $t_h = 0.04$ m and vertical walls thickness $t_v = 0.05$ m and is identical to the box-shaped cross section studied by Murín and Kutiš [6]. Throughout the entire numerical example the geometric constants of the bar are assumed to take the values presented in [6] ($A = 0.240$ m^2, $I_t = 0.089824$ m^4, $I_t^S = 0.001107$ m^4, $C_S = 0,000193$ m^6), while the results have been obtained employing 31 nodal points (longitudinal discretization). The bar's left end is clamped, while its right end is free and subjected to zero axial load, zero warping moment and prescribed twisting moment ($N(l,t) = 0, M_w(l,t) = 0, M_t(l,t) = \overline{M_t}$).

In the beginning, for comparison purposes, the linear static loading conditions are investigated by dropping all the inertia and nonlinear terms of (19), (20). A concentrated twisting moment $\overline{M_t} = 32$ kN m is applied at the bar's right end and the computed results of several kinematical and stress components taking into account or ignoring the STMDE are presented in Table 6 as compared wherever possible with those obtained from a FEM solution [6]. The coincidence of the results between the proposed and the FE methods is remarked. Moreover, from the comparison of the results obtained considering or ignoring the STMDE, it is concluded that STMDE influences decisively the stress components, while it exhibits a less pronounced effect on the kinematical components. Thus, the significance of STMDE in linear static analysis of bars of closed shaped cross sections, already reported in the literature [6], is verified.

Following the linear static loading conditions, the linear forced vibrations are investigated by dropping all the nonlinear terms of (19), (20). More specifically, the resonance of the examined bar is studied by applying a distributed twisting moment $m_{t,\mathrm{ext}}$ at $0 < x < 5$ (m) given as $m_{t,\mathrm{ext}}(x,t) = m_{t0}\sin(\omega_{f,\mathrm{lin}}t)$, where $m_{t0} = 5$ kN m/m and $\omega_{f,\mathrm{lin}} = 835.793$ s^{-1} ($M_t(l,t) = 0$, vanishing initial conditions $\bar{\theta}_{x0}(x) = 0$, $\dot{\bar{\theta}}_{x0}(x) = 0$). $\omega_{f,\mathrm{lin}}$ is the fundamental natural frequency of the bar undergoing linear torsional vibrations, ignoring STMDE and is numerically evaluated by performing modal analysis as this is presented in [63]. In Fig. 12 the time histories of the secondary twisting moment $M_t^S(0,t)$ at the bar's left end taking into account or ignoring (scaled quantity $M_t^S(0,t) \times 0,1$) the STMDE are presented demonstrating the decisive influence of the aforementioned effect to this stress resultant. Finally, in Fig. 13 the time histories of the warping moment $M_w(0,t)$ at the bar's left end are depicted taking into account or ignoring the STMDE. From Figs. 12, 13, the conclusions already drawn from Table 6 concerning static analysis can be extended in linear dynamic analysis of bars of closed shaped cross sections.

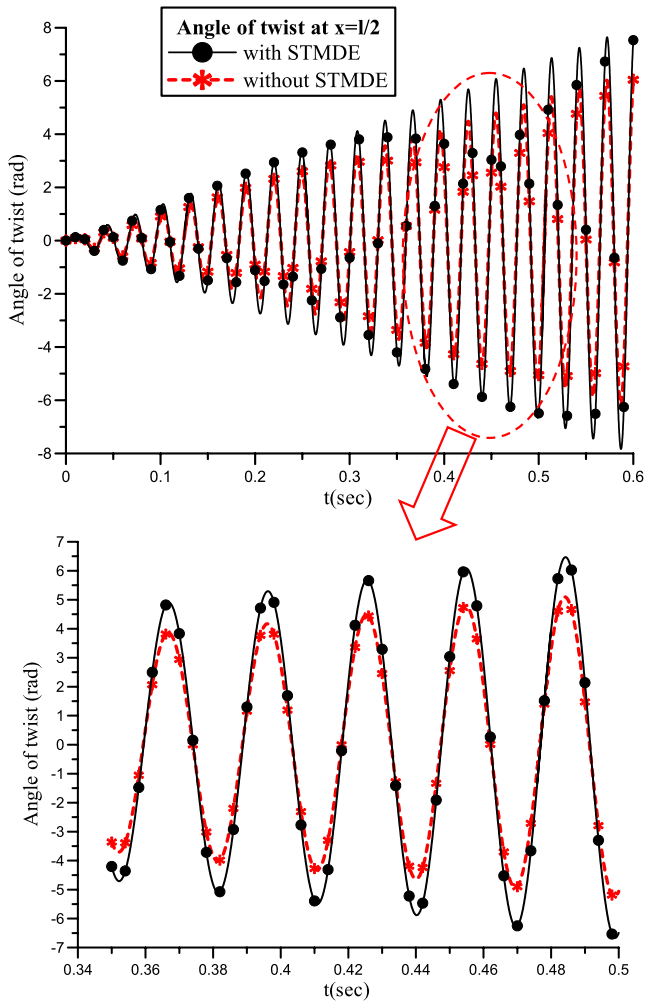

Fig. 9 Time histories of the angle of twist at the midpoint of the bar of Example 3 taking into account or ignoring secondary twisting moment deformation effect—geometrically linear case

5 Concluding remarks

In this paper a boundary element method is developed for the nonuniform torsional vibration problem of simply or multiply connected cylindrical bars of arbitrary doubly symmetric cross section, taking into account the effects of geometrical nonlinearity and secondary twisting moment deformation. The displacement components are expressed so as to be valid for large twisting rotations (finite displacement—small strain theory), while the use of an independent warping parameter makes it possible to account for warping shear stresses in global equilibrium of the bar. The main conclusions that can be drawn from this investigation are

a. The numerical technique presented in this investigation is well suited for computer aided analysis of cylindrical bars of arbitrarily shaped doubly symmetric cross section, supported by the most general twisting and warping boundary conditions and subjected to the combined action of arbitrarily distributed or concentrated time dependent conservative axial and torsional loading.
b. The geometrical nonlinearity leads to coupling between the torsional and axial equations of motion and alters the modeshapes of vibration. Consequently, the initiation of small amplitude free vibrations of buckled bars with the linear fundamental modeshape as initial twisting rotations induces higher harmonics in the bar's response, but its fundamental natural frequency is only slightly affected.
c. Large twisting rotations have a profound effect on both the positions around which vibrations are performed and the fundamental natural frequency of

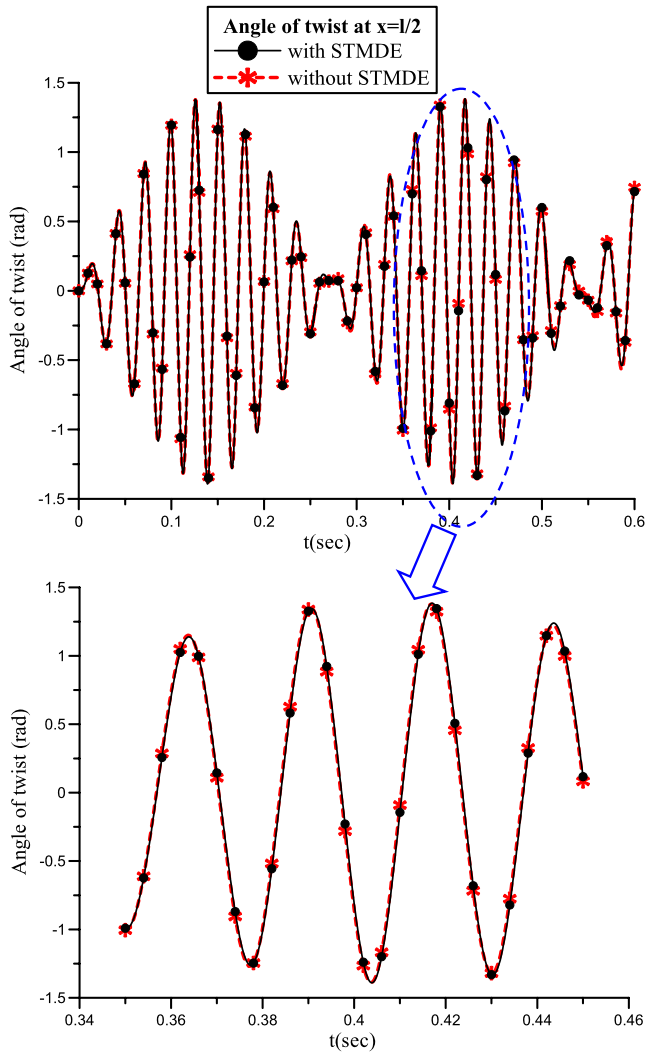

Fig. 10 Time histories of the angle of twist at the midpoint of the bar of Example 3 taking into account or ignoring secondary twisting moment deformation effect—geometrically nonlinear case

Table 5 Extreme values of various kinematical and stress components of the bar of Example 3, obtained for $0.00 \leq t \leq 0.30$ (s)

	With STMDE	Without STMDE
$\max \theta_x(l/2)$ (rad)	1.378	1.376
$\min \theta_x(l/2)$ (rad)	−1.393	−1.388
$\max M_t^P(0)$ (kN m)	17.407	17.359
$\min M_t^P(0)$ (kN m)	−17.555	−17.537
$\max M_{t,\mathrm{lin}}^S(0)$ (kN m)	12.464	12.205
$\min M_{t,\mathrm{lin}}^S(0)$ (kN m)	−12.318	−12.491
$\max M_{t,\mathrm{nl}}(0)$ (kN m)	19.199	18.887
$\min M_{t,\mathrm{nl}}(0)$ (kN m)	−19.690	−19.474
$\max M_t(0)$ (kN m)	49.070	48.427
$\min M_t(0)$ (kN m)	−49.545	−49.499

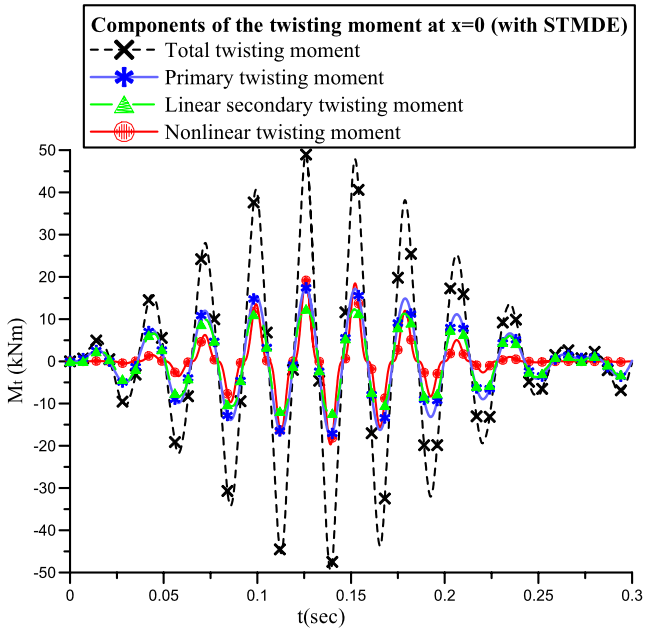

Fig. 11 Time histories of various twisting moment components at the left end of the bar of Example 3 taking into account the secondary twisting moment deformation effect (geometrically nonlinear analysis)

Table 6 Kinematical and stress components for linear static loading conditions of the bar of Example 4, taking into account or ignoring the secondary twisting moment deformation effect

	With STMDE				Without STMDE	
	$x=0$		$x=l$		$x=0$	$x=l$
	FEM [6]	Present study—AEM	FEM [6]	Present study—AEM	Present study–AEM	
M_t^P (Nm)	31, 610.4	31, 610.2	31,999.5	31,999.5	0	32,000.1
M_t^S (Nm)	389.6	389.6	0.5	0.5	32,000.0	−0.1
M_w (Nm^2)	−263.95	−264.14	0	0	−2,397.12	0
θ_x (rad)	0	0	2.20×10^{-5}	2.20×10^{-5}	0	2.17×10^{-5}
$\eta_x (m^{-1})$[a]	0	0	4.40×10^{-6}	4.41×10^{-6}	0	4.41×10^{-6}

[a]When STMDE is ignored, $\eta_x = \theta_x'$

buckled bars undergoing large amplitude free vibrations. The computation of dynamic characteristics of buckled bars differs from the one of bars at a pre-buckled state where the increase of initial amplitude of vibration always leads to an increase of the fundamental natural frequency.

d. The natural frequency of the axial displacement's response of buckled bars undergoing large amplitude free vibrations is twice as much as the one of the twisting rotation's one, when vibrations are performed around the static equilibrium position of the prebuckling configuration.
e. As expected, geometrical nonlinearity bounds the (twisting) deformations of bars at a pre-buckled state subjected to primary resonance excitations. A beating phenomenon is observed in the time histories of kinematical and stress components.
f. The secondary twisting moment deformation affects negligibly the kinematical and stress components of bars of open shaped thin-walled cross sections undergoing free or forced vibrations of small or large amplitude.
g. The secondary twisting moment deformation affects the kinematical components of bars of closed shaped cross sections undergoing linear vibrations. Its effect is much more pronounced on stress components, concluding that it cannot be neglected in

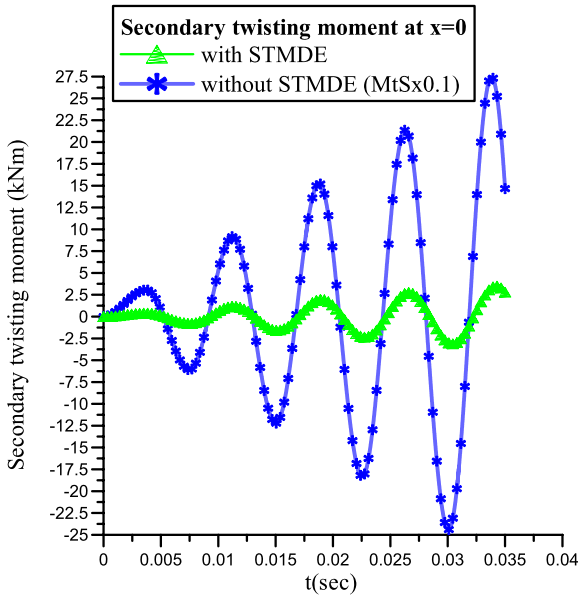

Fig. 12 Time histories of the secondary twisting moment $M_t^S(0,t)$ taking into account or ignoring (scaled quantity) the secondary twisting moment deformation effect at the left end of the bar of Example 4

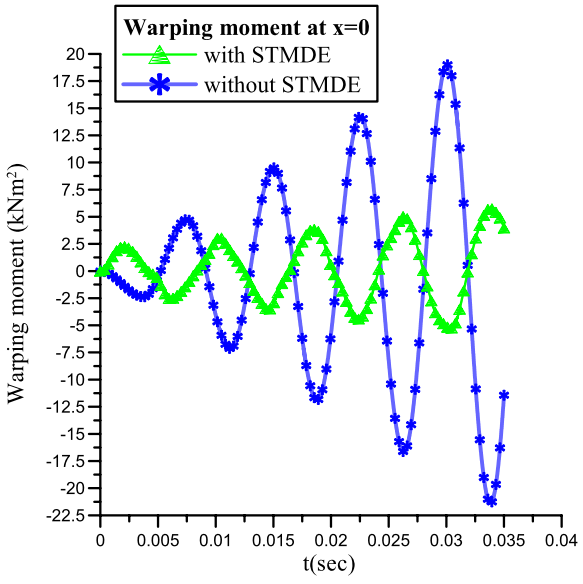

Fig. 13 Time histories of the warping moment $M_w(0,t)$ taking into account or ignoring the secondary twisting moment deformation effect at the left end of the bar of Example 4

linear dynamic analysis of bars of such cross sections.

The developed procedure retains most of the advantages of a BEM solution over a FEM approach, although it requires longitudinal domain discretization.

Appendix

Expression of the primary torsion constant I_t: Substituting (4) into (9a), the primary torsion constant of (10a) is obtained as

$$I_t = \int_\Omega \left[\left(\frac{\partial \phi_S^P}{\partial y} - z \right)^2 + \left(\frac{\partial \phi_S^P}{\partial z} + y \right)^2 \right] \mathrm{d}\Omega = I_1 + I_2 \tag{A.1}$$

where

$$I_1 = \int_\Omega \left(y^2 + z^2 + y \frac{\partial \phi_S^P}{\partial z} - z \frac{\partial \phi_S^P}{\partial y} \right) \mathrm{d}\Omega \tag{A.2a}$$

$$I_2 = \int_\Omega \left[\frac{\partial \phi_S^P}{\partial y} \left(\frac{\partial \phi_S^P}{\partial y} - z \right) + \frac{\partial \phi_S^P}{\partial z} \left(\frac{\partial \phi_S^P}{\partial z} + y \right) \right] \mathrm{d}\Omega \tag{A.2b}$$

Carrying out suitable integration by parts with respect to y for the first term of (A.2b) and with respect to z for the second term of (A.2b) and exploiting both (6a) and (6b), I_2 is proved to vanish. Consequently, I_t is proven to be given from expression (10a).

Expression of the secondary torsion constant I_t^S: Substituting (5) into (9a), the secondary torsion constant of (10b) is obtained as

$$I_t^S = A_\theta \int_\Omega \left[\left(\frac{\partial \phi_S^P}{\partial y} \right)^2 + \left(\frac{\partial \phi_S^P}{\partial z} \right)^2 \right] \mathrm{d}\Omega \tag{A.3}$$

Carrying out suitable integration by parts with respect to y for the first term of (A.3) and with respect to z for the second term of (A.3) and exploiting (8), I_t^S is written as

$$I_t^S = A_\theta \int_\Gamma \phi_S^P \frac{\partial \phi_S^P}{\partial n} \mathrm{d}s \tag{A.4}$$

or by exploiting (6b)

$$I_t^S = A_\theta \int_\Gamma \phi_S^P (z n_y - y n_z) \mathrm{d}s \tag{A.5}$$

Using the Gauss divergence theorem, (A.5) yields the exact formula of (10b).

Finally it is worth here noting that the alternative definitions of M_t^P, M_t^S as

$$M_t^P = \int_\Omega \left[S_{xy}^P(-z) + S_{xz}^P y\right] \mathrm{d}\Omega \tag{A.6a}$$

$$M_t^S = \int_\Omega \left[S_{xy}^S(-z) + S_{xz}^S y\right] \mathrm{d}\Omega \tag{A.6b}$$

can be easily proven to be identical to the ones presented in (9a), (9a).

Acknowledgements The authors would like to thank the Senator Committee of Basic Research of the National Technical University of Athens, Programme "PEVE-2008", R.C. No: 65 for the financial support of this work.

References

1. Sapountzakis, E.J., Mokos, V.G.: Warping shear stresses in nonuniform torsion by BEM. Comput. Mech. **30**, 131–142 (2003)
2. Simo, J.C., Vu-Quoc, L.: A geometrically-exact rod model incorporating shear and torsion-warping deformation. Int. J. Solids Struct. **27**, 371–393 (1991)
3. Sapountzakis, E.J., Tsipiras, V.J.: Warping shear stresses in nonlinear nonuniform torsional vibrations of bars by BEM. Eng. Struct. **32**, 741–752 (2010)
4. Schulz, M., Filippou, F.C.: Generalized warping torsion formulation. J. Eng. Mech. **124**, 339–347 (1998)
5. Vlasov, V.: Thin-walled elastic beams. Israel Program for Scientific Translations, Jerusalem (1963)
6. Murín, J., Kutis, V.: An effective finite element for torsion of constant cross-sections including warping with secondary torsion moment deformation effect. Eng. Struct. **30**, 2716–2723 (2008)
7. Sapountzakis, E.J., Mokos, V.G.: Secondary torsional moment deformation effect by BEM. In: Proceedings of the 10th International Conference of Advances in Boundary Element Techniques, Athens, Greece, pp. 81–88 (2009)
8. El Fatmi, R.: Non-uniform warping including the effects of torsion and shear forces. Part I: A general beam theory. Int. J. Solids Struct. **44**, 5912–5929 (2007)
9. El Fatmi, R.: Non-uniform warping including the effects of torsion and shear forces. Part II: Analytical and numerical applications. Int. J. Solids Struct. **44**, 5930–5952 (2007)
10. Kim, N., Kim, M.: Exact dynamic/static stiffness matrices of non-symmetric thin-walled beams considering coupled shear deformation effects. Thin-Walled Struct. **43**, 701–734 (2005)
11. Back, S.Y., Will, K.M.: A shear-flexible element with warping for thin-walled open beams. Int. J. Numer. Methods Eng. **43**, 1173–1191 (1998)
12. Chen, H., Blandford, G.E.: A C0 finite element formulation for thin-walled beams. Int. J. Numer. Methods Eng. **28**, 2239–2255 (1989)
13. Hu, Y., Jin, X., Chen, B.: A finite element model for static and dynamic analysis of thin-walled beams with asymmetric cross-sections. Comput. Struct. **61**, 897–908 (1996)
14. Saadé, K., Espion, B., Warzée, G.: Non-uniform torsional behavior and stability of thin-walled elastic beams with arbitrary cross sections. Thin-Walled Struct. **42**, 857–881 (2004)
15. Gendy, A.S., Saleeb, A.F., Chang, T.Y.P.: Generalized thin-walled beam models for flexural-torsional analysis. Comput. Struct. **42**, 531–550 (1992)
16. Laudiero, F., Savoia, M.: Shear strain effects in flexure and torsion of thin-walled beams with open or closed cross-section. Thin-Walled Struct. **10**, 87–119 (1990)
17. Laudiero, F., Savoia, M.: The shear strain influence on the dynamics of thin-walled beams. Thin-Walled Struct. **11**, 375–407 (1991)
18. Prokic, A., Lukic, D.: Dynamic analysis of thin-walled closed-section beams. J. Sound Vib. **302**, 962–980 (2007)
19. Kollár, L.P.: Flexural-torsional vibration of open section composite beams with shear deformation. Int. J. Solids Struct. **38**, 7543–7558 (2001)
20. Park, S., Fujii, D., Fujitani, Y.: A finite element analysis of discontinuous thin-walled beams considering nonuniform shear warping deformation. Comput. Struct. **65**, 17–27 (1997)
21. Cortinez, V.H., Piovan, M.T.: Vibration and buckling of composite thin-walled beams with shear deformability. J. Sound Vib. **258**, 701–723 (2002)
22. Machado, S.P., Cortínez, V.H.: Free vibration of thin-walled composite beams with static initial stresses and deformations. Eng. Struct. **29**, 372–382 (2007)
23. Minghini, F., Tullini, N., Laudiero, F.: Vibration analysis with second-order effects of pultruded FRP frames using locking-free elements. Thin-Walled Struct. **47**, 136–150 (2009)
24. Vo, T.P., Lee, J.: Flexural-torsional coupled vibration and buckling of thin-walled open section composite beams using shear-deformable beam theory. Int. J. Mech. Sci. **51**, 631–641 (2009)
25. Da Silva, M.: Non-linear flexural-flexural-torsional-extensional dynamics of beams—I. Formulation. Int. J. Solids Struct. **24**, 1225–1234 (1988)
26. Da Silva, M.: Non-linear flexural-flexural-torsional-extensional dynamics of beams—II. Response analysis. Int. J. Solids Struct. **24**, 1235–1242 (1988)
27. Pai, P.F., Nayfeh, A.H.: Three-dimensional nonlinear vibrations of composite beams—I. Equations of motion. Nonlinear Dyn. **1**, 477–502 (1990)
28. Pai, P.F., Nayfeh, A.H.: Three-dimensional nonlinear vibrations of composite beams—II. Flapwise excitations. Nonlinear Dyn. **2**, 1–34 (1991)
29. Pai, P.F., Nayfeh, A.H.: Three-dimensional nonlinear vibrations of composite beams—III. Chordwise excitations. Nonlinear Dyn. **2**, 137–156 (1991)
30. Di Egidio, A., Luongo, A., Vestroni, F.: A non-linear model for the dynamics of open cross-section thin-walled beams—Part I: formulation. Int. J. Non-Linear Mech. **38**, 1067–1081 (2003)
31. Di Egidio, A., Luongo, A., Vestroni, F.: A non-linear model for the dynamics of open cross-section thin-walled beams—Part II: forced motion. Int. J. Non-Linear Mech. **38**, 1083–1094 (2003)
32. Pai, P.F., Nayfeh, A.H.: A fully nonlinear theory of curved and twisted composite rotor blades accounting for warpings

and three-dimensional stress effects. Int. J. Solids Struct. **31**, 1309–1340 (1994)
33. Avramov, K.V., Galas, O.S., Morachkovskii, O.K., Pierre, C.: Analysis of flexural-flexural-torsional nonlinear vibrations of twisted rotating beams with cross-sectional deplanation. Strength Mater. **41**, 200–208 (2009)
34. Rozmarynowski, B., Szymczak, C.: Non-linear free torsional vibrations of thin-walled beams with bisymmetric cross-section. J. Sound Vib. **97**, 145–152 (1984)
35. Sapountzakis, E.J., Tsipiras, V.J.: Nonlinear nonuniform torsional vibrations of bars by the boundary element method. J. Sound Vib. **329**, 1853–1874 (2010)
36. Szymczak, C.: Buckling and initial post-buckling behavior of thin-walled I columns. Comput. Struct. **11**, 481–487 (1980)
37. Emam, S.A., Nayfeh, A.H.: Nonlinear responses of buckled beams to subharmonic-resonance excitations. Nonlinear Dyn. **35**, 105–122 (2004)
38. Emam, S.A., Nayfeh, A.H.: On the nonlinear dynamics of a buckled beam subjected to a primary-resonance excitation. Nonlinear Dyn. **35**, 1–17 (2004)
39. Nayfeh, A., Emam, S.: Exact solution and stability of postbuckling configurations of beams. Nonlinear Dyn. **54**, 395–408 (2008)
40. Emam, S.A., Nayfeh, A.H.: Postbuckling and free vibrations of composite beams. Compos. Struct. **88**, 636–642 (2009)
41. Mohri, F., Azrar, L., Potier-Ferry, M.: Vibration analysis of buckled thin-walled beams with open sections. J. Sound Vib. **275**, 434–446 (2004)
42. Katsikadelis, J.T.: The analog equation method. A boundary-only integral equation method for nonlinear static and dynamic problems in general bodies. Theor. Appl. Mech. **27**, 13–38 (2002)
43. Chen, G., Trahair, N.: Inelastic nonuniform torsion of steel I-beams. J. Constr. Steel Res. **23**, 189–207 (1992)
44. Machado, S.P., Cortínez, V.H.: Lateral buckling of thin-walled composite bisymmetric beams with prebuckling and shear deformation. Eng. Struct. **27**, 1185–1196 (2005)
45. Ramm, E., Hofmann, T.J.: Stabtragwerke, Der Ingenieurbau. In: Mehlhorn, G. (ed.) Band Baustatik/Baudynamik. Ernst & Sohn, Berlin (1995)
46. Rothert, H., Gensichen, V.: Nichtlineare Stabstatik. Springer, Berlin (1987)
47. Brush, D.O., Almroth, B.O.: Buckling of Bars, Plates and Shells. McGraw-Hill, New York (1975)
48. Trahair, N.S.: Nonlinear elastic nonuniform torsion. J. Struct. Eng. **131**, 1135–1142 (2005)
49. Armenakas, A.E.: Advanced Mechanics of Materials and Applied Elasticity. Taylor & Francis, New York (2006)
50. Sapountzakis, E.J.: Torsional vibrations of composite bars by BEM. Compos. Struct. **70**, 229–239 (2005)
51. Timoshenko, S.P., Goodier, J.N.: Theory of Elasticity. McGraw-Hill, New York (1970)
52. Sapountzakis, E.J.: Solution of non-uniform torsion of bars by an integral equation method. Comput. Struct. **77**, 659–667 (2000)
53. Rubin, H.: Wölbkrafttorsion von Durchlaufträgern mit konstantem Querschnitt unter Berücksichtigung sekundärer Schubverformungen. Stahlbau **74**, 826–842 (2005)
54. Kraus, M.: Computerorientierte Bestimmung der Schubkorrekturfaktoren gewalzter I-Profile. In: Festschrift Rolf Kindmann, pp. 81–98. Shaker Verlag, Aachen (2007)
55. Sapountzakis, E., Dourakopoulos, J.: Flexural-torsional buckling analysis of composite beams by BEM including shear deformation effect. Mech. Res. Commun. **35**, 497–516 (2008)
56. Sapountzakis, E., Dourakopoulos, J.: Shear deformation effect in flexural–torsional vibrations of beams by BEM. Acta Mech. **203**, 197–221 (2009)
57. Sapountzakis, E., Dourakopoulos, J.: Nonlinear dynamic analysis of Timoshenko beams by BEM. Part I: Theory and numerical implementation. Nonlinear Dyn. **58**, 295–306 (2009)
58. Prokic, A.: On fivefold coupled vibrations of Timoshenko thin-walled beams. Eng. Struct. **28**, 54–62 (2006)
59. Sapountzakis, E.J., Mokos, V.G.: Nonuniform torsion of bars of variable cross section. Comput. Struct. **82**, 703–715 (2004)
60. Brigham, E.: Fast Fourier Transform and Its Applications. Prentice Hall, New Jersey (1988)
61. Mohri, F., Azrar, L., Potier-Ferry, M.: Flexural-torsional post-buckling analysis of thin-walled elements with open sections. Thin-Walled Struct. **39**, 907–938 (2001)
62. Bhashyam, G., Prathap, G.: Galerkin finite element method for non-linear beam vibrations. J. Sound Vib. **72**, 191–203 (1980)
63. Sapountzakis, E., Mokos, V.: Dynamic analysis of 3-D beam elements including warping and shear deformation effects. Int. J. Solids Struct. **43**, 6707–6726 (2006)